

Homologues of Radial Spoke Head Proteins Interact with Ca²⁺/Calmodulin in *Tetrahymena* Cilia

Hironori Ueno*, Yoshinori Iwataki and Osamu Numata[†]

Graduate School of Life and Environmental Sciences, University of Tsukuba, Tsukuba, Ibaraki 305-8572

Received July 11, 2006; accepted August 22, 2006

Calmodulin (CaM) is an axonemal component. To examine the pathway of Ca²⁺/CaM signaling in cilia, using Ca²⁺/CaM-affinity column, we identified seven Ca²⁺/CaM-associated proteins from a crude dynein fraction and isolated 62 kDa (p62) and 66 kDa (p66) Ca²⁺/CaM-associated proteins in *Tetrahymena* cilia. The amino acid sequences deduced from the p62 and p66 cDNA sequences suggested that these proteins were similar to *Chlamydomonas* radial spoke proteins 4 and 6 (RSP4 and RSP6), components of the radial spoke head, and sea urchin sperm p63, which is a homologue of RSP4/6, and isolated as a key component that affect flagellar bending patterns. Although p62 and p66 do not have a conventional CaM-binding site, those have consecutive sequences which showed high normalized scores (≥ 5) from a CaM target database. These consecutive sequences were also found in RSP4, RSP6, and p63. These radial spoke head proteins have a high similarity region composed of 15 amino acids between the five proteins. Immunoelectron microscopy using anti-CaM antibody showed that CaM was localized along the outer edge of the curved central pair microtubules in axoneme. Therefore, it is possible that the interaction between Ca²⁺/CaM and radial spoke head control axonemal curvature in the ciliary and flagellar waveform.

Key words: calcium, calmodulin, cilia, flagella, radial spoke head, *Tetrahymena*.

Abbreviations: CaM, calmodulin; CP/RS, Central pair/radial spoke; DRC, dynein regulatory complex.

In various eukaryotic organisms, cilia and flagella are universal organelle, which possess fine structure comprised of nine doublet microtubules and two central pair microtubules. Many kinds of eukaryotic cilia and flagella change their waveform in response to the internal Ca²⁺ concentration. In the reactivated cell models of *Paramecium*, an increase in Ca²⁺ concentration induced reversal of swimming direction by changing the direction of the ciliary effective stroke (1). The biflagellate green alga *Chlamydomonas reinhardtii* also displays a marked Ca²⁺-dependent waveform conversion (2). When axoneme isolated from sea urchin sperm were reactivated in vitro under low calcium conditions, those axonemes beat with a symmetric waveform. Upon increasing calcium concentration in the buffer, the axonemes beat with increasing asymmetry (3); at extremely high calcium concentrations, quiescence was induced (4).

CaM has been identified as a component of ciliary and flagellar axonemes of various eukaryotic cells (5, 6). In *Chlamydomonas*, axonemal CaM located in the radial spoke stalk (7) and the C1a projection of central pair structure (8). The radial spokes are T-shape structures extending from the A-tubule of each outer doublet microtubule to the central pair structure of the axoneme, adjacent to the

inner dynein arms and two or three of them are arranged within each 96-nm repeat. The *Chlamydomonas* radial spoke contains at least 23 proteins, 18 of which have been characterized at the molecular level (9). Some spoke stalk proteins are predicted to have domains associated with signal transduction, including CaM-, Ca²⁺-, AKAP- and nucleotide-binding domains. RSP2 (118 kDa radial spoke protein) has structural homologues of the “1-8-14” Ca²⁺-dependent CaM binding motifs, including both type B and type A (10). These motifs are based on the conserved residues at positions 1, 8, and 14 in the amphipathic helical structure (11). Moreover, RSP23 (102 kDa radial spoke protein), which consists of an N-terminal nucleoside diphosphate kinase (NDK) catalytic module and a C-terminal domain containing three IQ motifs that bind CaM, is an integral component of the radial spoke stalk (12). Recently, in central pair structure, it is reported that CaM is a component of the C1a complex (8). In central pair-less *Chlamydomonas* strains, flagella become paralyzed (13). However, flagellar motility can be restored by the introduction of a suppressor mutation in components of the dynein arms or the dynein regulatory complex (DRC) (14–16). It implicates that the central pair structure also plays an important role to modulate ciliary and flagellar waveform by regulating dynein activity. The radial spoke heads are made up of five proteins in *Chlamydomonas*; these transiently interact with the central pair projection (17). Structural and genetic analyses showed that radial spokes and their interactions with the central pair apparatus play a crucial role in regulation of ciliary and flagellar motility and waveform (18, 19). For example, in *Chlamydomonas*, failure to assemble

[†]To whom correspondence should be addressed. Tel: +81-29-853-6648, Fax: +81-29-853-6614, E-mail numata@sakura.cc.tsukuba.ac.jp

*Present address: Research Institute for Cell Engineering, National Institute for Advanced Industrial Science and Technology, Tsukuba Central 4, 1-1-1 Higashi, Tsukuba, Ibaraki 305-8562.

the radial spokes results in flagellar paralysis, even though their axonemes are capable of sliding disintegration (13). However, at low ATP concentrations (< 100 μ M), CP/RS-deficient axonemes are capable of beating and the waveform conversion occurred at $\geq 10^{-5}$ M Ca^{2+} concentration, although the waveform is different between the mutants and the wild type (20). Huang *et al.* isolated extragenic suppressor mutations that bypassed the requirement for the radial spoke and/or the central pair (14). These genes, which caused suppressor mutations, encode seven proteins known as the DRC (15). The DRC contains at least seven polypeptides that are tightly associated with the outer doublet microtubules (16). The DRC has also been associated with a crescent-shaped structure located near the base of the second radial spoke, close to the site of attachment for the nexin link (21). In studies with the demembrated/reactivated sperm model of sea urchin, it was reported that monoclonal antibody D-316 caused transformation of the flagellar waveform, but the beat frequency was unaffected by dose. The protein recognized by D-316 is related to RSP4 and RSP6, which are radial spoke head proteins of *Chlamydomonas* (22). Moreover, it suggests that Ca^{2+} controls dynein activity by a regulatory mechanism of the CP/RS complex (23). In Triton-extracted models of *Paramecium*, trifluoperazine (TFP), a CaM antagonist, can inhibit the ciliary reversal in the presence of cyclic adenosine 3',5'-monophosphate (cAMP) (24). We focused on role of Ca^{2+} /CaM in cilia; we researched Ca^{2+} /CaM binding-proteins in *Tetrahymena* cilia. Though elongation factor 1 α (EF-1 α), a Ca^{2+} /CaM-binding protein, has been isolated from the membrane and matrix fraction of *Tetrahymena* cilia (25), a biochemical isolation of the Ca^{2+} /CaM target proteins in the crude dynein fraction had not been performed.

In this study, to examine the pathway of Ca^{2+} /CaM signaling in *Tetrahymena* cilia, we identified target proteins of Ca^{2+} /CaM in the crude dynein fraction of cilia using Ca^{2+} /CaM-affinity column chromatography. The crude dynein fraction included outer and inner arm dyneins, radial spokes and central pair structures. We detected 120 kDa (p120), 116 kDa (p116), 66 kDa (p66), 62 kDa (p62), 33 kDa (p33), and 30 kDa (p30-1, p30-2) Ca^{2+} /CaM-associated proteins in this fraction. Two main Ca^{2+} /CaM-associated proteins among them, p62 and p66, were separated with 2D-SDS-PAGE; corresponding cDNAs were cloned and the amino acid sequences were analyzed. p62 and p66 were homologue of *Chlamydomonas* or sea urchin radial spoke head proteins, which regulate flagellar bending patterns. The results suggest that, as the target proteins of Ca^{2+} /CaM, p62 and p66 were involved in the regulation mechanism of flagellar bending pattern.

MATERIALS AND METHODS

Cell Culture—Cultivation of *Tetrahymena thermophila* (B24964WT) was performed as described previously (26).

Isolation and Fractionation of Cilia—Isolation of axonemes was performed as described in our previous study (25). The crude dynein fraction was prepared as follows. The axoneme was washed with Tris-Mg solution (2 mM MgSO_4 , 30 mM Tris-HCl, pH 8.3), and dialyzed against a Tris-EDTA solution (0.1 mM EDTA, 1 mM Tris-HCl,

pH 8.0) for 3 h, and centrifuged at $10,000 \times g$ for 20 min. The supernatant is referred to as the "crude dynein fraction."

Affinity Purification of Ca^{2+} /CaM-Associated Proteins from the Crude Dynein Fraction—Affinity purification of Ca^{2+} /CaM-associated proteins from the crude dynein fraction was performed using two different methods. First, the GST-CaM bound glutathione-sepharose 4B (Amersham Pharmacia Biotech, USA) was incubated with the crude dynein fraction in binding buffer (1 mM CaCl_2 , 40 mM KCl, 2 mM MgSO_4 , 20 mM Tris-HCl, pH 7.5) for 100 min at 4°C. The beads were then loaded into a Poly-Prep Column (Bio-Rad, USA) and washed with washing buffer (1 mM CaCl_2 , 100 mM KCl, 2 mM MgSO_4 , 20 mM Tris-HCl, pH 7.5). GST-CaM-associated proteins were eluted with buffer (5 mM EGTA, 100 mM-1 M KCl, 2 mM MgSO_4 , 20 mM Tris-HCl, pH 7.5). GST bound glutathione-sepharose 4B was used as a control column. Second, preparation of a GST-CaM affinity column and control GST column were carried using the HiTrap NHS-activated (Amersham Biosciences Europe GmbH, Freiburg, Germany), according to the manufacturer's instructions. GST-CaM (5 mg/1 ml) was applied to a HiTrap NHS-activated sepharose column (column volume 1 ml). Coupling of GST to the HiTrap NHS-activated was carried out in the same manner. Each 10 ml of crude dynein fraction was applied to a GST-CaM column or a control GST column equilibrated with binding buffer (1 mM CaCl_2 , 40 mM KCl, 2 mM MgSO_4 , 20 mM Tris-HCl, pH 7.5) at a flow rate of 0.1 ml/min. After loading, each column was rinsed with binding buffer containing 100 mM KCl at 1 ml/min for 120 min. Then the columns were eluted successively with elution buffer (5 mM EGTA, 100 mM KCl, 2 mM MgSO_4 , and 20 mM Tris-HCl, pH 7.5).

Cloning of p62 and p66 Proteins—The p62 and p66 Ca^{2+} /CaM-associated proteins spots were cut from a 2D-SDS-PAGE gel, digested by lysyl endopeptidase, and fractionated on a high performance liquid chromatography (HPLC) using reverse-phase column. Micro sequencing of the derived peptides was performed by APRO Life Science Institute (Naruto, Tokushima, Japan). Sequences of two peptides, (K)TPYPGDTENEPP from the p62 protein and (K)LVDPEDATGRTL from the p66 protein, were obtained. These sequences were used to search the *T. thermophila* genomic DNA database at TIGR (The Institute for Genomic Research, Rockville, MD, USA) using BLAST (Basic Local Alignment Search Tool). DNA sequences encoding these peptides were found from scaffold DNA. The genes, ID 8254437 and ID 8254671, encoded polypeptides in (K)TPYPGDTENEPP from p62 and (K)LVDPEDATGRTL from p66, respectively (Fig. 3, A and C). Open reading frames of these regions were estimated by BLAST search at NCBI (National Center for Biotechnology Information, Bethesda, MD, USA). RNA was isolated from mid-log phase *T. thermophila* using Isogen (Nippon Gene, Tokyo, Japan) according to the manufacturer's protocol. First strand cDNA synthesis was performed with SMART RACE cDNA Amplification Kit (BD Biosciences Clontech, Palo Alto, CA, USA). The polymerase chain reaction (PCR) and the rapid amplification of cDNA ends (RACE) were performed using first strand cDNA as template DNA. For RACE amplification, primers 5'-GGGGGTAATAAA-GGCAATTCATCC-3' (5'-RACE for p62), 5'-CTCCAAAA-

CCTACACCTGCCCATTC-3' (5'-RACE for p66), 5'-GCT-TTGGATGACCCTGAAAACCCAATC-3' (3'-RACE for p62), and 5'-ACCCAGAAGATGCAACTGGCCGTACT-3' (3'-RACE for p66) were used with the manufacturer's primers. PCR was performed using cDNA library as template DNA. PCR products were cloned into T vectors (Qiagen, San Diego, CA, USA) and we determined the cDNA sequences with an ABI PRISM 310 (Applied Biosystems, USA). Homologous proteins were searched at Genome Net (Kyoto University Bioinformatics Center, Kyoto, Japan) using BLAST search. Multiple alignments of homologous proteins were calculated by CLUSTAL W Multiple Sequence Alignment Program (version 1.8) at Genome Net.

Other Procedures—An affinity-purified rabbit anti-*Tetrahymena* CaM antibody was prepared in our previous study (27). Immunoelectron microscopy was performed as described in our previous study (25). Isoelectric focusing with Immobiline DryStrip (Amersham Pharmacia Biotech, Uppsala, Sweden) was performed for the first dimension of 2D electrophoresis as described (28). SDS-PAGE was carried out according to the method of Laemmli (29). The protein concentration was determined by the method of Bradford with bovine serum albumin as standard (30).

RESULTS

Identification of Ca^{2+} /CaM-Associated Proteins in Crude Dynein Fraction—In immunoelectron microscopy using anti-CaM antibody, most of the immunogold particles for

CaM were observed in the region between the central pair microtubules and the outer doublet microtubules (25). Since radial spokes existed in this region, we expected that components of radial spokes would bind to a Ca^{2+} /CaM-affinity column. *Tetrahymena* cilia were sequentially extracted by detergent, dialysis against low ionic strength, and dialysis against high ionic strength. These extracted samples were analyzed by SDS-PAGE and silver staining (Fig. 1B). We refer to the low ionic strength dialysis fraction as the "crude dynein fraction," including outer and inner arm dyneins, radial spoke and central pair structures. To search for Ca^{2+} /CaM-associated proteins in the crude dynein fraction, we performed Ca^{2+} /CaM-affinity column chromatography using an NHS-activated HiTrap column. Using this column, we succeeded in obtaining the seven Ca^{2+} /CaM-associated proteins (Dynein heavy chain, p120, p116, p66, p62, p33, and p30) in quantities sufficient for further analysis (Fig. 1E). We regard the high molecular weight protein as probably being the heavy chains of dynein. To investigate the direct interaction of CaM and dynein, we isolated mixture of 14S and 22S dynein from *Tetrahymena* cilia, and applied on the Ca^{2+} /CaM-affinity column prepared with NHS-activated HiTrap column. As a result, dynein did not interact directly with Ca^{2+} /CaM (data not shown). Thus, it suggested that interaction of CaM and dynein was mediated by the other Ca^{2+} /CaM-associated protein(s). Moreover, p120 and p116 Ca^{2+} /CaM-associated proteins are probably homologues of *Chlamydomonas* RSP2 and RSP23 with molecular weights were 118 and 102 kDa in SDS-PAGE, respectively. It has been reported that RSP2 and RSP23 have CaM-binding

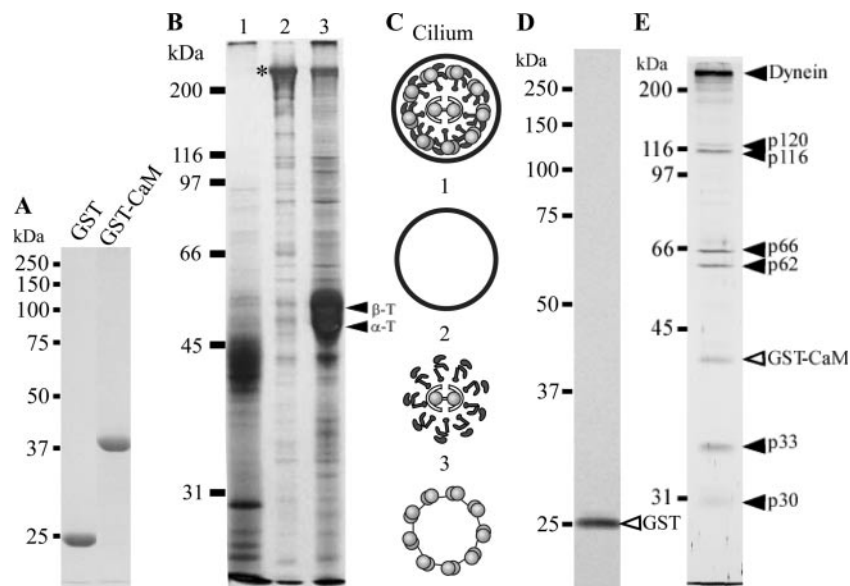


Fig. 1. Ca^{2+} /CaM-associated proteins in crude dynein fraction. (A) GST-CaM fusion protein used for CaM-affinity column and GST alone for the control column. (B) Fractionation of *Tetrahymena* cilia was performed as following. Axonemes were sequentially treated as follows, incubation with 1% Triton X-100 for 10 min at 4°C (lane 1), dialysis against low ionic strength buffer for 3 h at 4°C (lane 2), and dialysis against high ionic strength buffer for overnight at 4°C (lane 3). Aliquots of fractions collected at each step were electrophoresed on 10% SDS-polyacrylamide gels and the proteins were stained with silver staining. A high molecular weight protein in lane 2 is dynein (asterisk). (C) Schematic

diagrams show axonemal structure expected to be included in each fraction. (D, E) Ca^{2+} /CaM-associated proteins in the crude dynein fraction. Ca^{2+} /CaM-associated proteins were eluted from a GST-CaM affinity column (E) and a GST control column (D) with elution buffer containing 5 mM EGTA and 100 mM KCl. Closed arrowheads indicate dynein heavy chain, 120, 116, 66, 62, 33, and 30 kDa Ca^{2+} /CaM-associated proteins, and open arrowheads indicate GST-CaM and GST from the ligand. The gels were silver-stained. The apparent molecular weights (kDa) are shown on the left.

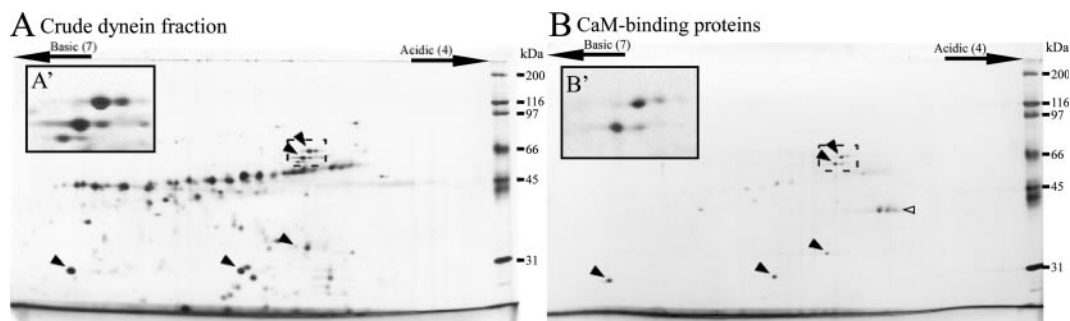


Fig. 2. 2D-SDS-PAGE gels of crude dynein fraction and Ca^{2+} /CaM-associated proteins in crude dynein fraction. (A) 2D-SDS-PAGE pattern of crude dynein fraction. (B) 2D-SDS-PAGE pattern of Ca^{2+} /CaM-associated proteins eluted from a HiTrap GST-CaM affinity column with elution buffer containing 5 mM EGTA and 100 mM KCl. Proteins were revealed by silver staining. The apparent molecular weights (kDa) are shown on the right.

The acid end of the gel is to the right. Closed arrowheads indicate 66, 62, 33, and 30 kDa Ca^{2+} /CaM-associated proteins, and open arrowhead indicates GST-CaM from the ligand. Two Ca^{2+} /CaM-associated proteins were contained in the 30 kDa fraction. Insets (A') and (B'), higher magnification view of p62 and p66 region indicates by dotted line boxes in (A) and (B).

motifs (10, 12). Since the other molecular weight proteins (p66, p62, p33, and p30) have not been reported, we focused on these proteins.

2D-SDS-PAGE Analysis of Ca^{2+} /CaM-Associated Proteins—To confirm whether Ca^{2+} /CaM-associated proteins obtained by binding assay exist in the crude dynein fraction, we examined compared by 2D SDS-PAGE spots in the crude dynein fraction with those in the Ca^{2+} /CaM-associated proteins. As a result, we found the spots of p66, p62, p33, and p30 in crude dynein fraction (Fig. 2). The spots of p66 and p62 in the crude dynein fraction were slightly shifted to the acidic side. These shifted spots also bound to the Ca^{2+} /CaM-affinity column (Fig. 2, A' and B'). In addition, the amount of p33 spot in the crude dynein fraction was very small. However, the amount of the p33 spot among the Ca^{2+} /CaM-associated proteins increased compared with that in the crude dynein fraction. We suggest that this protein strongly binds to Ca^{2+} /CaM. In the case of p30, there were two spots at 30 kDa, showing that 30 kDa Ca^{2+} /CaM-associated proteins contained two proteins, p30-1 and p30-2. Therefore, there were 7 Ca^{2+} /CaM-associated proteins (p120, p116, p66, p62, p33, p30-1, and p30-2) in the crude dynein fraction.

Molecular Cloning and Sequence Analysis of p62 and p66—The spots of p62 and p66 in the crude dynein fraction were major spots compared with the other spots, and slightly shifted to the acidic side. Several research groups suggested that the Ca^{2+} /CaM-dependent enzymes were involved in ciliary and flagella waveform (24, 31). Therefore, it is possible that p62 and p66 are also involved in ciliary and flagellar waveform. The spots of p62 and p66 were transferred to polyvinylidene fluoride (PVDF) membrane, stained with Coomassie Brilliant Blue, and then analyzed with a protein sequencer. However, the N-termini of p62 and p66 were protected with post-translational modifications. To determine inner-amino acid sequences, p62 and p66 were isolated from 2D-SDS-PAGE gels, and were digested to peptides with lysyl-endopeptidase. These peptides were separated by HPLC, and amino acid sequences were determined (Material and Methods). Amino acid sequences of peptide from p62 and p66 were (K)TPYPGDTENEPP and (K)LVDPE-DATGRTL, respectively. The genes encoding the peptide sequences were searched from among the genome DNA

sequence database of *Tetrahymena thermophila* for genomic DNA sequences at TIGR. We found the genomic DNA encoding the amino acid sequences of these peptides in the database. These open reading frames were predicted from the BLAST search. For getting cDNAs of p62 and p66, PCR, 5'-RACE and 3'-RACE were performed using first strand cDNA as template DNA (Materials and Methods). Consequently, complete cDNA sequences of p62 and p66 were determined (Fig. 3, A and C). Since amino acid sequences estimated from these cDNAs included peptide sequences of p62 and p66, respectively, we concluded that these cDNAs encode *Tetrahymena thermophila* p62 and p66. p62 and p66 were 463 and 493-amino acid proteins and their molecular weights 53.5 and 56.9 kDa, respectively (Fig. 3). The molecular weight of each protein was smaller than that estimated from the electrophoretic mobility, suggesting that the three dimensional structures of these proteins may be flexible structure.

Sequence Analyses of p62 and p66—BLAST homology search of p62 and p66 revealed identities to radial spoke head proteins including *Chlamydomonas* RSP4 and RSP6. p62 is homologous to RSP6 with 30% identity and 50% similarity and RSP4 with 27% identity and 45% similarity. p66 also had homology to RSP4 and RSP6 with 24% identity and 38% similarity to both. Secondary structure analysis predicted that p62 and p66 have a coiled-coil region in the open reading frame from approximately residues 310 to 350 and residues 50 to 100, respectively (Fig. 3E). On the other hand, sea urchin radial spoke head protein p63 has two coiled-coil regions in one sequence (Fig. 3F). Though p62 and p66 do not have a conventional CaM-binding site, these proteins have consecutive sequences that showed high normalized scores (≥ 5) from a CaM target database (<http://calcium.uhnres.utoronto.ca/ctdb/flash.htm>). The normalized scores were evaluated with the following criteria: hydrophathy, alpha-helical propensity, residue weight, residue charge, hydrophobic residue content, helical class, and occurrence of particular residues. A high valued consecutive string indicates the location of a putative CaM-binding site. Since normalized scores of the amino acid residues 138–157 in p62 and 136–155 in p66 were ≥ 5 , those residues were probably CaM-binding sites (Fig. 3F). The length of the putative CaM-binding sites in p62 and p66 were 20

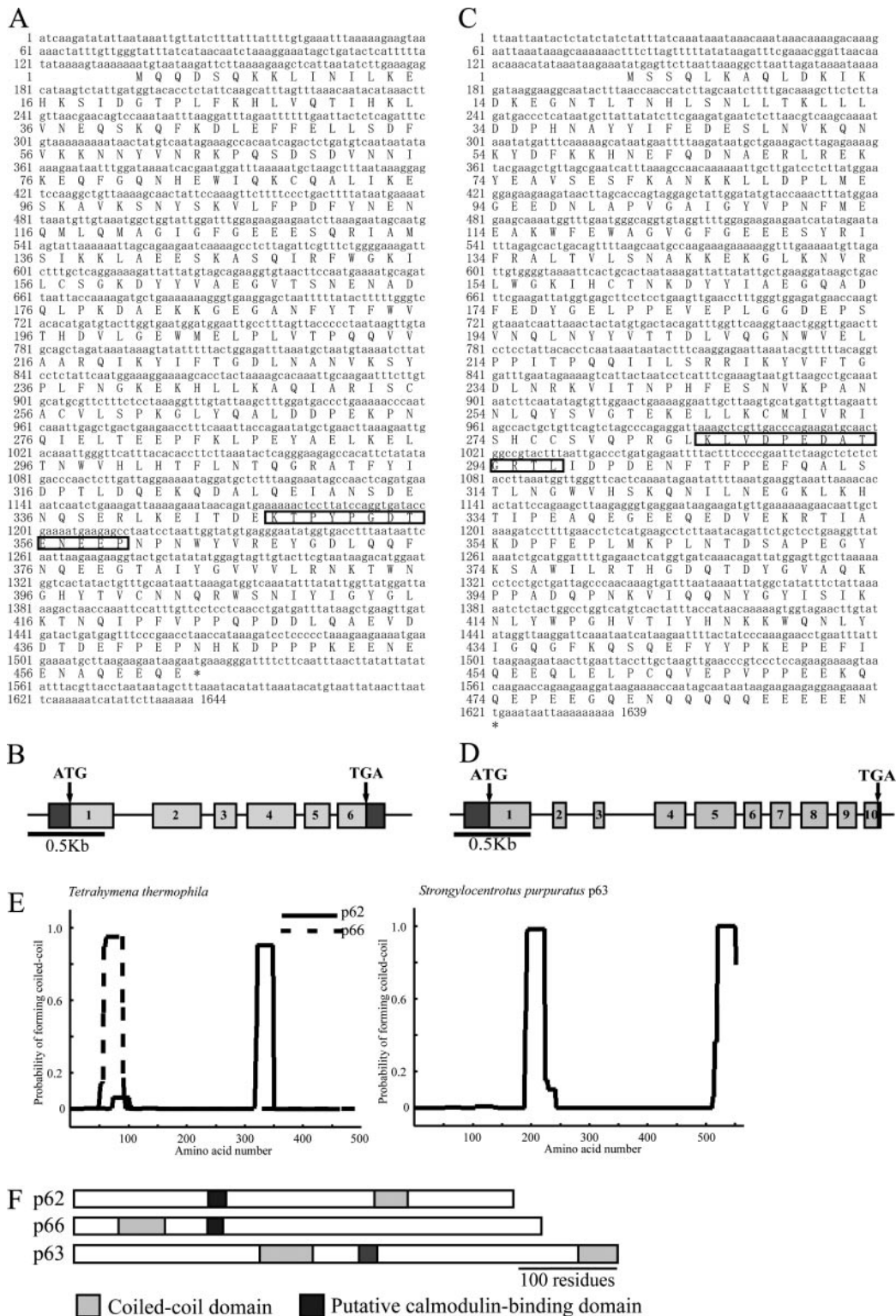


Fig. 3. Nucleotide and deduced amino acid sequences, coiled coil domain, and putative CaM-binding domains in p62 and p66. (A) and (C) Nucleotide and deduced amino acid sequences of full-length cDNAs that encode p62 and p66. Boxed areas denote the regions of determined amino acid sequences. Open reading frames of p62 and p66 consist of 463 and 493 amino acids, respectively. (B and D) Exon-intron maps. Exons are shown in boxes. (E) Coiled-coil domains of p62, p66, and radial spoke head protein p63 of *Strongylocentrotus purpuratus* were predicted according to the program

COILS (44). Probability of coiled-coil formation was calculated by a 28-residue window. (F) Schematic diagrams of predicted secondary structures of p62, p66 and p63 are represented schematically, using open boxes. Gray boxes indicate coiled-coil domains. Black boxes indicate putative CaM-binding domains. Analysis of CaM-binding domain performed by a program for prediction of CaM-binding site (http://calcium.uhnres.utoronto.ca/ctdb/pub_pages/search/index.htm). Black boxes indicates consecutive strings with high normalized scores (≥ 5).

Cr RSP4	1	-----MAAVDSVAQALAYLVQHSPQDGT	
Cr RSP6	1	-----MAADVQALAFLLQVKTQGA	
Sp p63	1	MMEEPQNEGTPKTKGNSKPQTPTGTAVATPPNMAVNLTPTEALVNAKAYLLKASNKSNL	
Tt p62	1	-----MQQDSQKLLINILKEHKSIDGT	
Tt p66	1	-----MSSQLKAQLDKIKDKEGN	
			: * . . .
Cr RSP4	24	SMYDHLVKLVSQVLEDPKNAVLDLLETSLLVKSTFDPKKESPLVPIPVAPDATQTQAAV	
Cr RSP6	22	SIYEGLKAALAKVLEDRPVNAVEALETSVLSTPPAAN--LSVPLVPAASAAAAAATAVAKA	
Sp p63	61	NLYDHLSRILTKVLDERPENVVDLFDISKVVKSKFTSTSDTILDKVDKTAEVELGETQ	
Tt p62	23	PLFKHLVQTIHKLVEQSKQFKDLEFFELLSDFFVKKNYVNRKPSDSVNNIKKQFQGN	
Tt p66	19	TLTNHLSNLLTKLLDDPHNAYYIFEDFSLNVKQNKYDFKHKHNEFQDNAERI.REKYEAVS	
		: . * : * : . . .	
Cr RSP4	84	SIFGDPELPIPATGEPVADPPN--EFEAENMLGAAVLDCLGVGLGRELGVNIALAAK	
Cr RSP6	80	SLFGDPEPVLDPESGEPIDPDAPN--EFECEDVEGDGLDGLGVGLGRQEMAYAAVLAVK	
Sp p63	121	KILFER--DQEEAEHDGGEDEV--ETPLPNLPELMYHFEQAGVGVSRREEMRIYLAK	
Tt p62	83	HEWIKQCALIKES--KAVKSNYS--KVLFPDFYNENQMLQMGIFGFEESQRISAMIK	
Tt p66	79	<u>ESFKANKKLLDPLMEGFEDNLPVGAIGYVVPNFMEAKWFVWAGVGFEEESYRIFRALI</u>	
		: . : : * : . . .	
Cr RSP4	142	RIGEDPK-LAVRSVRFKFLGLYSDYFVFEVAFKK-----EAAKE	
Cr RSP6	138	<u>RLGEDAK-RGVSTVRFKFGKFFGTADYVFFETLQS-----NPDMP</u>	
Sp p63	175	QLVDN--YPLQSCRFWGKLEKTEKNIYVAEVEYREGHEEEEEHEETEPDEKDEE	
Tt p62	139	KLAAE--SKASQIRFWGKLLCSGRDYVAEGVTSN-----	
Tt p66	139	VLSNAKKEKGLKNVRLWGIHCTNKDYYIAEQGADFEDYG-----	
		: : : * : * : * : *	
Cr RSP4	182	AAPAAPAPERVEGEAASSAPEVPEEPKGANFKTYLVCSSLGG-PLTRLPDVTPAQVK	
Cr RSP6	178	EAPEG-----TIPLEPYGEGVNAVYIFVSNLTLGG-PLQQLPYVTPEQIK	
Sp p63	232	<u>EGEGEEQEEEDLKPDPFKPPVIPREENRTGNTKKTFFVCNEPGQ-PWVKLPAITPLQIS</u>	
Tt p62	172	-----ENADQLPKDAEKKGEGANFYTFWVTHDVLG--EWMELPLVTPQQVV	
Tt p66	179	-----ELPPEVEPLGGDEPSVNLNYYVTTDLVQGNVWELPPIPTQQII	
		. . * : * : * : * : *	
Cr RSP4	241	<u>ASRRIKKLLTGRLLTSHVSTYPAFP-----GNEANYLRALARTSAATVVAPS</u>	
Cr RSP6	221	ASRLRLRYLTGRLLDAPVSAFPAPF-----GNEANYLRALIARISAATVCCPR	
Sp p63	291	<u>VARQIKKFFTGRLLDQQLISYPPFN-----GTEANYLRAQISRVSAQTQISPL</u>	
Tt p62	216	AARQIKYIFTGDLNANVKSYPFLN-----GKEKHLKKAQIARISACACVLSPK	
Tt p66	223	LSRRIKYVFTGDLNRKVIINPHFESNVKANNLQYSV <u>GTEKELLKCMIVRIS</u> HCCSVQPR	
		: * : : * * * : : * * * * * * *	
Cr RSP4	288	DLFSLNDETGERA-----EDWEPPAGREMAAPTAWVHVRPHLKSQGRCEVHK	
Cr RSP6	268	GFFTADDDSAELSAN-----DEWVPLKREMALPVNWSHRYAHLKGGQRTVTHK	
Sp p63	338	GFYQFDEEEEEEDGNRDSFIESPDFEGIPVKDLVDPMSANWVHHVQHILPQGRCSWFN	
Tt p62	263	GLYQALDDPEKPNQIELT-----EEPFKLPEYAKELKELTNVHLHTFLNTQGRATFYI	
Tt p66	283	GLKLVDPEDATGRLLIDP-----DENFTFPEFQALSTLNGVHHSKQNILNEGLKHTI	
		: . : : * * : : *	
Cr RSP4	337	-----RELPEDAEDE--FYNEDELEEGPDLLAALEEDAQLPGEQ-----AAWTP--	
Cr RSP6	317	-----RDPDEEEPEKFWTAEMEAGPPPLATLDTDAPLPAATGDKVPPPAWSP--	
Sp p63	398	PVQQEEDFEDEDEEEREPEPEPEVGPPLLTPLSEDEVENIP-----PWS---	
Tt p62	316	<u>DP-----TLDQEKQDALQEIANDENQSERLKEITDEKTPYPGDTENEENPNVYVREY</u>	
Tt p66	336	PEAQ--EGEEQEDVEKRTIAKDPFEPLMKPLNTDSAPEGYKSAWILRTHGDQTDYGVAAQ	
		: . .	
Cr RSP4	380	----IYSSASEAVKTAAGLRLSLVWPGAVCGGRGSEWTCVYVWGKVN--APFVPLPP	
Cr RSP6	368	----VFASASVTRNQVAGVRSNRWPGAVCACAGRHTSMYVWGVIKAGGEWSPCPPPPP	
Sp p63	447	----ARLTSSLVPQYATAVIQSNLWPGAYAFGTDKKFNENVYIGWGHKYSY--DNYSPPPP	
Tt p62	370	GDLQFNFQEEGTAYGVVVLRNKTWNGHYTVCCNQRWSNIYIGYGLKTN--QIPFVPPQP	
Tt p66	393	KPPADQPNKVIQQNYGYSIKNLYWPGHVTIYHNKKNQNLVIGQGFKQSQ--EFYYPKEP	
		: . : * * : : * * * * * * *	
Cr RSP4	432	PPVAQEFAGW-----EVETQELELKPAPPPPEEEAAEAD-----	
Cr RSP6	424	VPQWGAPAAG-----VEGGQQLLLECNLDLPKPAPEEEDE-----	
Sp p63	501	PPVQEEFSPGPEITAEADPTPEEEAALAAQQEAMEAAEEMEDEEEEDGEDD--	
Tt p62	428	DDLQAEVDDT-----DEFPEPNHKDPPKPEENEENAQEEQE-----	
Tt p66	451	EFIQEEQLELP-----CQVEPVPPPEEKQPEEGQENQQQQE-----	
		: : : * : : *	

amino acid residues each (Fig. 3F). Sequence comparison of p62 and p66 with RSP6 indicates that the putative CaM-binding sites of these three proteins have been conserved in the same position (Fig. 4). p63 has two coiled-coil structures and a putative CaM-binding site that has been conserved in the same position as that in RSP4

(Fig. 4). However, RSP4 and RSP6 do not have coiled-coil regions (Fig. 4). The boxed region represents the 15-amino acid sequence with high similarity between the four proteins (Fig. 4); that sequence is also conserved with sea urchin radial spoke head protein p63 that was involved in the regulation of sperm beat pattern (22).

Fig. 4. Clustal W alignment of the deduced amino acid sequences of p62 and p66, shown with the sequences of *Chlamydomonas* RSP4, RSP6, and *Strongylocentrotus* p63. “*” indicates positions with identical amino acid residues. “:” is divided into the “strong” group. “.” is classified as the “weaker” group. The strong and weak groups are defined as strong score >0.5 and weak score ≤0.5. These score was calculated by the Gonnet Pam250 matrix. Putative CaM-binding domains are denoted with shaded residues. The boxed region represents the sequence with high similarity between all five proteins. The residues indicated by underlines represent predicted coiled-coil domain of p62, p66, and p63. The GenBank accession numbers for the proteins Cr RSP4, Cr RSP6, Sp p63, Tt p62, and Tt p66 are Q01656, Q01657, NP999761, ABB03904, and ABB03905, respectively. Cr, *Chlamydomonas reinhardtii*; Sp, *Strongylocentrotus purpuratus*; Tt, *Tetrahymena thermophila*.

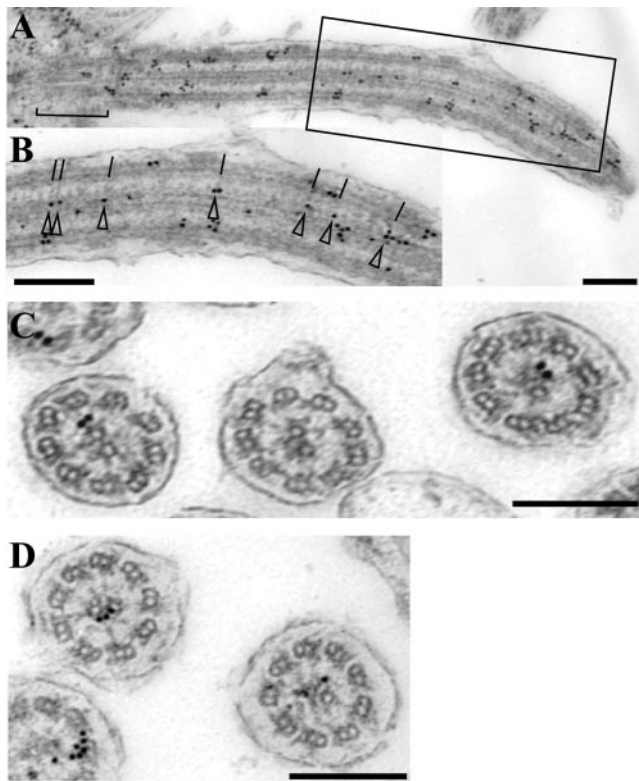


Fig. 5. **Immunoelectron micrographs for CaM in *Tetrahymena* cilia.** (A) Micrographs of longitudinal section of a curved cilium. Localization of CaM was at the basal body (bracket) and the entire length of cilia. (B) Higher magnification view of curved cilium region indicated by the box in A. Localization of CaM was observed on the outer doublet microtubules and along the outer edge of the curved central pair microtubule (arrowhead). Inclining radial spokes structure are able to be observed (lines). (C and D) Transverse section of cilia. CaM localized near the center of axoneme. Bar = 200 nm.

Localization of CaM in Tetrahymena Cilia—Immunoelectron microscopy using anti-CaM antibody showed that immunogold particles for CaM was found on the base of the radial spoke in *Tetrahymena* (25). However, we were able to observe that some immunogold particles for CaM were found on the center of the axoneme in longitudinal and transverse sections (Fig. 5). The signals on the outer doublet microtubules probably result from binding between CaM and EF-1 α (25). Interestingly, in curved cilium region, inclining radial spokes were observed (Fig. 5B, lines), and most of the CaM in the center of the axoneme was localized along the outer edge of the curved central pair microtubules (Fig. 5B, arrowheads). Few immunogold particles were found at random in control experiments with a rabbit preimmune serum or secondary antibody alone (data not shown).

DISCUSSION

In this study, using Ca²⁺/CaM-affinity column chromatography, p120, p116, p66, p62, p33, p30-1, and p30-2 were identified as Ca²⁺/CaM-associated proteins in the crude dynein fraction of *Tetrahymena* cilia. In 2D SDS-PAGE, the spots of p62 and p66 in the crude dynein fraction

are slightly shifted to the acidic side relative to their positions in a gel made with Ca²⁺/CaM-associated proteins. It is possible that these spot shifts are caused by post-translational modification, such as phosphorylation. Since previous studies have reported that some axonemal proteins were phosphorylated in a Ca²⁺/CaM-dependent manner (32), these post translational modifications are thought to play a key role in the stimulation of ciliary motility. Ca²⁺/CaM-dependent kinase and various types of phosphatases anchored to the axoneme seem to be important in ciliary or flagellar motility (31). In addition, cAMP is known to be required for the initiation and maintenance of axonemal motility in sperm (33) and *Paramecium* (34). Specific inhibitors of protein kinase A (PKA) alter motility of ATP-induced reactivated movement of ciliary and flagellar axonemes (35, 36).

Since p62 and p66 were major spots compared with the other Ca²⁺/CaM-associated proteins, we focused on p62 and p66, and cloned the cDNA of these proteins. Molecular cloning of the cDNA encoding these proteins revealed that p62 and p66 were homologues of radial spoke head proteins. However, molecular weights of the proteins encoded by these cDNAs were lower than those calculated from the electrophoretic mobility in SDS-PAGE. Interestingly, this discrepancy has also been observed for the other radial spoke head proteins (22, 37). These proteins may have intrinsic structural features that reduce their mobility in SDS-PAGE. In these cases, it has been suggested that the helix containing proline was found to be strongly kinked, causes the flexible formation in protein structure (38).

Sequence comparison of *Tetrahymena* radial spoke head proteins with RSP4/6 and sea urchin radial spoke head protein p63 indicates that a 15-amino acid sequence has been particularly conserved throughout evolution (Fig. 4). It is reported that the near this amino acid sequence is the highest similarity between the sea urchin p63, *Chlamydomonas* RSP4 and RSP6 (22). Since this sequence is also conserved in other species such as *Homo sapiens* and *Mus musculus* (Radial Spokehead-like 1), this sequence may be essential to the function of radial spoke heads. Moreover, *Tetrahymena* spoke head proteins form coiled-coil structures in the C-terminal side of p62 and the N-terminal side of p66 (Figs. 3 and 4). Though *Chlamydomonas* RSP4 and RSP6 do not have the coiled-coil structures, spoke head proteins of sea urchin have two coiled-coil structures (Figs. 3 and 4). The coiled-coil structures may play a role in the formation of flexible lateral domains that extend toward the central pair projection. Difference of coiled-coil structures may reflect the difference of movement such as the waveform or amplitude of *Tetrahymena* cilia, sea urchin sperm flagella and *Chlamydomonas* flagella.

In analysis of *Chlamydomonas* mutants, it was suggested that radial spokes, the central pair and the dynein regulatory complex are involved in the regulation of dynein-driven microtubule sliding (39), possibly by phosphorylation of a regulatory inner arm component (40, 41). The structure and function of the radial spoke complex have been analyzed using *Chlamydomonas* motility mutants with paralyzed flagella (pf). RSP1, 4, 6, 9, and 10 are encoded by separate genes and a single mutation in RSP4 (pf1), RSP9 (pf17), or RSP6 (pf26) results in the

absence of the entire spoke head structure and the flagellar paralysis. In cross sections, the radial spoke heads transiently interacted with the central pair projections (17). Since flagella become paralyzed when radial spoke heads are missing, it was thought that radial spoke heads received some signal from the central pair structure by transient interaction with the central pair projections. The transient interaction may be a key event in regulation of dynein activity. Since the central apparatus and radial spoke in *Chlamydomonas* were regulated by $\text{Ca}^{2+}/\text{CaM}$ and CaM -dependent kinase II, $\text{Ca}^{2+}/\text{CaM}$ -binding proteins in the central apparatus and radial spoke were key components of the Ca^{2+} signaling pathway (31).

In our study, p62 and p66 were identified as $\text{Ca}^{2+}/\text{CaM}$ -associated proteins, and were homologues of radial spoke head proteins. Immunoelectron micrographs showed that CaM localized near the radial spoke head (Fig. 5), suggesting that $\text{Ca}^{2+}/\text{CaM}$ bind to p62 and p66 in the radial spoke head. Moreover, we have much interest in the CaM localization along the outside of the central pair microtubules in curved region (Fig 5B). Because, it is reported that the central pair microtubules always curves with C1 facing the outside (42), and CaM is a component of the C1a complex (8). Since it is thought that the waveform conversion of cilia and flagella relates to the curvature of axoneme, it is possible that the interaction between $\text{Ca}^{2+}/\text{CaM}$ and radial spoke head control axonemal curvature in the waveform.

Moreover, p62 and p66 were possibly phosphorylated. The axoneme contains some A-kinase anchoring protein and CaM -dependent kinase (31, 43). In *Chlamydomonas*, two axonemal A-kinase anchoring proteins have been identified in the central pair apparatus and the radial spoke stalk (43), and the calcium-induced increase in dynein activity was inhibited by antagonists of CaM and CaM -dependent kinase II in central pair-less *Chlamydomonas* strains (31). Therefore, there is a possibility that A kinase and CaM -dependent kinase take part in the phosphorylation of p62 and p66. From the above-mentioned, we posit that p62 and p66 induce change of ciliary movement by receiving $\text{Ca}^{2+}/\text{CaM}$ signaling and phosphorylation-dephosphorylation signaling in the radial spoke head. On the other hand, several other $\text{Ca}^{2+}/\text{CaM}$ -associated proteins (p120, p116, p33, p30-1, and p30-2) were identified. Characterization of p120, p116, p33, and p30-1, and p30-2 is an interesting subject for future study. In other future studies, identification of p66- and p62-binding proteins is important for demonstrating interaction between radial spoke and central pair.

In light of our studies, we suggest that $\text{Ca}^{2+}/\text{CaM}$ may regulate the interaction between radial spoke head and central pair structure and control axoneme curvature in the ciliary and flagellar waveform. These studies support a new model in which p62 and p66 in the radial spoke head play a role like the sensor of Ca^{2+} signaling. Interaction of $\text{Ca}^{2+}/\text{CaM}$ with p62 and p66 in the radial spoke head may trigger specific calcium-induced changes that affect ciliary and flagellar motility, by mechanisms including altered waveform.

Contract grant sponsor: Ministry of Education, Sciences, Sports and Culture of Japan; contract grant number: 10213201. We

thank all members of Numata's laboratory for helpful discussions and advice. We also thank Dr. Richard S. J. Weisburd for a critical reading of and helpful comments regarding the manuscript.

REFERENCES

- Naitoh, Y. and Kaneko, H. (1972) Reactivated triton-extracted models of *paramecium*: modification of ciliary movement by calcium ions. *Science* **176**, 523–524
- Hyams, J.S. and Borisy, G.G. (1978) Isolated flagellar apparatus of *Chlamydomonas*: characterization of forward swimming and alteration of waveform and reversal of motion by calcium ions in vitro. *J. Cell Sci.* **33**, 235–253
- Brokaw, C.J., Josslin, R., and Bobrow, L. (1974) Calcium ion regulation of flagellar beat symmetry in reactivated sea urchin spermatozoa. *Biochem. Biophys. Res. Commun.* **58**, 795–800
- Gibbons, H.B. and Gibbons, I.R. (1980) Calcium-induced quiescence in reactivated sea urchin sperm. *J. Cell Biol.* **84**, 13–27
- Gitelman, S.E. and Witman, G.B. (1980) Purification of calmodulin from *Chlamydomonas* occurs in cell bodies and flagella. *J. Cell Biol.* **98**, 764–770
- Stommel, E.W., Stephens, R.E., Masure, H.R., and Head, J.F. (1982) Specific localization of scallop gill epithelial calmodulin in cilia. *J. Cell Biol.* **92**, 622–628
- Yang, P., Diener, D.R., Rosenbaum, J.L., and Sale, W.S. (2001) Localization of calmodulin and dynein light chain LC8 in flagellar radial spokes. *J. Cell Biol.* **153**, 1315–1325
- Wargo, M.J., Dymek, E.E., Smith, E.F. (2005) Calmodulin and PF6 are components of a complex that localizes to the C1 microtubule of the flagellar central apparatus. *J. Cell Sci.* **118**, 4655–4665
- Yang, P., Diener, D.R., Yang, C., Kohno, T., Pazour, G.J., Dienes, J.M., Agrin, N.S., King, S.M., Sale, W.S., Kamiya, R., Rosenbaum, J.L., and Witman, G.B. (2006) Radial spoke proteins of *Chlamydomonas* flagella. *J. Cell Sci.* **119**, 1165–1174
- Yang, P., Yang, C., and Sale, W.S. (2004) Flagellar radial spoke protein 2 is a calmodulin binding protein required for motility in *Chlamydomonas reinhardtii*. *Eukaryotic Cell* **3**, 72–81
- Rhoads, A.R. and Friedberg, F. (1997) Sequence motifs for calmodulin recognition. *FASEB J.* **11**, 331–340
- Patel-King, R.S., Gorbatyuk, O., Takebe, S., and King, S.M. (2004) Flagellar radial spokes contain a Ca^{2+} -stimulated nucleoside diphosphate kinase. *Mol. Biol. Cell* **15**, 3891–3902
- Witman, G.B., Plummer, J., and Sander, G. (1978) *Chlamydomonas* flagellar mutants lacking radial spokes and central tubules. *J. Cell Biol.* **76**, 729–747
- Huang, B., Ramanis, Z., and Luck, D.J.L. (1982) Suppressor mutations in *Chlamydomonas* reveal a regulatory mechanism for flagellar function. *Cell* **28**, 115–124
- Piperno, G., Mead, K., and Shestak, W. (1992) The inner dynein arms I2 interact with a “dynein regulatory complex” in *Chlamydomonas* flagella. *J. Cell Biol.* **118**, 1455–1463
- Piperno, G., Mead, K., LeDizet, M., and Moscatelli, A. (1994) Mutations in the “dynein regulatory complex” alter the ATP-insensitive binding sites for inner arm dyneins in *Chlamydomonas* axonemes. *J. Cell Biol.* **125**, 1109–1117
- Goodenough, U.W. and Heuser, J.E. (1985) Substructure of inner dynein arms, radial spokes, and the central pair/projection complex of cilia and flagella. *J. Cell Biol.* **100**, 2008–2018
- Warner, F.D. and Satir, P. (1974) The structural basis of ciliary bend formation: radial spoke positional changes accompanying microtubule sliding. *J. Cell Biol.* **63**, 35–63

19. Huang, B. (1986) *Chlamydomonas reinhardtii*: a model system for the genetic analysis of flagellar structure and motility. *Int. Rev. Cytol.* **99**, 181–215
20. Wakabayashi, K., Yagi, T., and Kamiya, R. (1997) Ca²⁺-dependent waveform conversion in the flagellar axoneme of *Chlamydomonas* mutants lacking the central-pair/radial spoke system. *Cell Motil. Cytoskelet.* **38**, 22–28
21. Gardner, L.C., O'Toole, E., Perrone, C.A., Giddings, T., and Porter, M.E. (1994) Components of a "dynein regulatory complex" are located at the junction between the radial spokes and the dynein arms in *Chlamydomonas* flagella. *J. Cell Biol.* **127**, 1311–1325
22. Gingras, D., White, D., Garin, J., Cosson, J., Huitorel, P., Zingg, H., Cibert, C., and Gagnon, C. (1998) Molecular cloning and characterization of a radial spoke head protein of sea urchin sperm axonemes: involvement of the protein in the regulation of sperm motility. *Mol. Biol. Cell* **9**, 513–522
23. Nakano, I., Kobayashi, T., Yoshimura, M., and Shingyoji, C. (2003) Central-pair-linked regulation of microtubule sliding by calcium in flagellar axonemes. *J. Cell Sci.* **116**, 1627–1636
24. Izumi, A. and Nakaoka, Y. (1987) cAMP-mediated inhibitory effect of calmodulin antagonists on ciliary reversal of *Paramecium*. *Cell Motil. Cytoskel.* **7**, 154–159
25. Ueno, H., Gonda, K., Takeda, T., and Numata, O. (2003) Identification of elongation factor-1alpha as a Ca²⁺/calmodulin-binding protein in *Tetrahymena* cilia. *Cell Motil. Cytoskel.* **55**, 51–60
26. Watanabe, Y., Numata, O., Kurasawa, Y., and Kato, M. (1994) Cultivation of *Tetrahymena* cells. In *Cell Biology* (Celis, J.E., ed.) Vol. 1, pp. 398–404 Academic Press, California
27. Gonda, K., Katoh, M., Hanyu, K., Watanabe, Y., and Numata, O. (1999) Ca²⁺/calmodulin and p85 cooperatively regulate an initiation of cytokinesis in *Tetrahymena*. *J. Cell Sci.* **112**, 3619–3626
28. Kojima, H., Watanabe, Y., and Numata, O. (1997) The dual functions of *Tetrahymena* citrate synthase are due to the polymorphism of its isoforms. *J. Biochem.* **122**, 998–1003
29. Laemmli, U.K. (1970) Cleavage of structure proteins during the assembly of the head of bacteriophage T4. *Nature* **227**, 680–685
30. Bradford, M.M. (1976) A rapid and sensitive method for the quantitation of microgram quantities of protein utilizing the principle of protein-dye binding. *Anal. Biochem.* **72**, 248–254
31. Smith, E.F. (2002) Regulation of flagellar dynein by calcium and a role for an axonemal calmodulin and calmodulin-dependent kinase. *Mol. Biol. Cell* **13**, 3303–3313
32. Hirano-Ohnishi, J. and Watanabe, Y. (1989) Ca²⁺/calmodulin-dependent phosphorylation of ciliary β -tubulin in *Tetrahymena*. *J. Biochem.* **105**, 858–860
33. Morisawa, M. and Okuno, M. (1982) Cyclic AMP induces maturation of trout sperm axoneme to initiate motility. *Nature* **295**, 703–704
34. Nakaoka, Y., Tanaka, H., and Oosawa, F. (1984) Ca²⁺-dependent regulation of beat frequency of cilia in *Paramecium*. *J. Cell Sci.* **65**, 223–231
35. Brokaw, C.J. (1987) Regulation of sperm flagellar motility by calcium and cAMP-dependent phosphorylation. *J. Cell Biochem.* **35**, 175–184
36. San Agustin, J.T. and Witman, G.B. (1994) Role of cAMP in the reactivation of demembrated ram spermatozoa. *Cell Motil. Cytoskel.* **27**, 206–218
37. Piperno, G., Huang, B., Ramanis, Z., and Luck, D.J.L. (1981) Radial spokes of *Chlamydomonas* flagella: polypeptide composition and phosphorylation of stalk components. *J. Cell Biol.* **88**, 73–79
38. Yun, R.H., Anderson, A., and Hemans, J. (1991) Proline in alpha-helix: stability and conformation studied by dynamics simulation. *Proteins* **10**, 219–228
39. Smith, E.F., and Sale, W.S. (1992) Regulation of dynein-driven microtubule sliding by radial spokes in flagella. *Science* **257**, 1557–1559
40. Howard, D.R., Habermacher, G., Glass, D.B., Smith, E.F., and Sale, W.S. (1994) Regulation of *Chlamydomonas* flagellar dynein by an axonemal protein kinase. *J. Cell Biol.* **127**, 1683–1692
41. Habermacher, G. and Sale, W. (1996) Regulation of a flagellar dynein by axonemal type-1 phosphatase in *Chlamydomonas*. *J. Cell Sci.* **109**, 1899–1907
42. David R. Mitchell and Masako Nakatsugawa (2004) Bend propagation drives central pair rotation in *Chlamydomonas reinhardtii* flagella. *J. Cell Biol.* **166**, 709–715
43. Gaillard, A.R., Diener, D.R., Rosenbaum, J.L., and Sale, W.S. (2001) Flagellar radial spoke protein 3 is an A-kinase anchoring protein (AKAP). *J. Cell Biol.* **153**, 443–448
44. Lupas, A., Van Dyke, M., and Stock, J. (1991) Predicting coiled coils from protein sequences. *Science* **252**, 1162–1164